Available online at www.sciencedirect.com
ScienceDirect
Mendeleev Commun., 2015, **25**, 304–306
Mendeleev Communications

Penetration of methane–oxygen flames through spherical and planar obstacles in a closed cylindrical reactor

Nikolai M. Rubtsov,*[a] Boris S. Seplyarskii,[a] Ideya M. Naboko,[b] Victor I. Chernysh,[a] Georgii I. Tsvetkov[a] and Kirill Ya. Troshin[c]

[a] *Institute of Structural Macrokinetics and Materials Science, Russian Academy of Sciences, 142432 Chernogolovka, Moscow Region, Russian Federation. Fax: +7 495 962 8025; e-mail: nmrubtss@mail.ru*
[b] *Joint Institute for High Temperatures, Russian Academy of Sciences, 127412 Moscow, Russian Federation*
[c] *N. N. Semenov Institute of Chemical Physics, Russian Academy of Sciences, 119991 Moscow, Russian Federation*

DOI: 10.1016/j.mencom.2015.07.026

The ignition of a dilute methane–oxygen mixture (total pressure, to 200 Torr) after a single obstacle can be observed markedly far from the obstacle surface. The use of meshed sphere as an obstacle leads to an increase in the distance of flame emergence behind the obstacle in comparison with a round opening; two or more close-meshed obstacles strongly suppress flame propagation.

Flame propagation in ducts and channels is important for identifying the criteria of flashback in ducts and safety applications in power generation, mining and petrochemical industries. The problem is also relevant to combustion of gas flowing into the crevice volumes of internal combustion engines.[1] The interaction between the flame and the local blockage caused by the presence of equipment and vessels provides local flame acceleration of the propagating flame front (FF).[2] The modeling of the influences of such local blockage on explosion was performed through laboratory-scale studies.[3,4] The effect of pressure waves generated by a flame on the formation of FF shape was reported.[5,6]

The interaction of chemical kinetics and heat and mass transfer processes due to turbulent mixing caused by obstacles in combination with momentum exchange processes could significantly accelerate flames to the limits where the damage of a volume in which the flame accelerates is expected.[6–12] Such an undesirable influence of obstacles inside the volume on flame acceleration has been investigated.[8–10]

However, at highly blocking obstacles, the flame acceleration can be explained[9,10] by not only the increase of turbulence, when the expanding flow passes the obstacle, but also 'by accumulation of free radicals behind the obstacle. The mixing of these radicals with the unburned gas makes the gas mixture highly explosive'.[9]

It was shown[13,14] that spark initiated flames of lean hydrogen–air mixtures at 1 atm propagated through meshed aluminum spherical obstacles with a mesh size of 0.04–0.1 mm^2. The flame of 15% H_2 in air accelerated after obstacle; acoustic gas perturbations occurred in the reactor; the smaller diameter of the spherical mesh caused the earlier occurrence of the acoustic perturbations. However, the FF of a stoichiometric natural gas–air mixture did not accelerate after the obstacle; acoustic perturbations were missing. Thus, the active centers of methane and hydrogen combustion, which determine flame propagation, have different chemical nature, namely, the termination of active intermediates on the obstacle surface contributes significantly to the interaction of FF with obstacles in the case of natural gas–air mixtures; *i.e.*, the role of active intermediates is very important in the process.

Here we report experimental results on flame propagation in a cylindrical channel with obstacles. The aim of the work was to study FF penetration through single round openings and close meshed obstacles and to estimate the effectiveness of the obstacles for methane flame suppression.

Flame propagation through a single obstacle in CH_4–oxygen mixtures is shown in Figure S1 (Online Supplementary Materials).[†] In Figure 1(*a*),(*b*) selected frames of flame propagation through the round opening d = 2.5 and 4 cm inserted into a planar obstacle of 14 cm in diameter recorded with the speed video camera are presented. The following remarkable peculiarities of the combustion process are revealed: the ignition after obstacle does not occur in

[†] The flame propagation of stoichiometric mixtures of methane with oxygen diluted with CO_2 and Kr at initial pressures 100–200 Torr and 298 K in a pumped out horizontal cylindrical quartz reactor 70 cm in length and 14 cm in diameter was investigated. The reactor was fixed in two stainless steel gateways at butt-ends (Figure S1) supplied with inlets for gas pumping and blousing and a safety shutter, which swung outward when the total pressure in the reactor exceeded 1 atm. A pair of spark ignition electrodes was located near the butt-end of the reactor. A spherical mesh consisted of two stainless steel hemispheres fastened by a spring, and it was placed in the center of the reactor. Meshed spheres with the diameters d = 8 (wire diameter of 0.3 mm, cell size of 0.3 mm^2), 10 (wire diameter of 0.35 mm, cell size of 0.5 mm^2) and 13 cm (wire diameter of 0.5 mm, cell size of 1 mm^2) were used. In other experiments, planar meshed stainless steel obstacles with d = 14 cm (either with a wire d = 0.3 mm, cell size of 0.5 mm^2; or with a wire d = 0.5 mm and a cell size of 0.1 mm^2) were placed vertically in the center of the reactor. Meshed spheres d = 4 cm (wire d = 0.1 mm, cell size of 0.15 mm^2) and d = 5 cm (wire d = 0.15 mm, cell size of 0.2 mm^2) inserted into a planar obstacle d = 14 cm were also used. For comparison, FF propagation through the planar obstacle with a central single round opening of 2.5 cm in diameter was investigated as the simplest model. The combustible mixture (15.4% CH_4 + 30.8% O_2 + + 46% CO_2 + 7.8% Kr) was prepared prior to experiment; CO_2 was added to decrease FF velocity and to enhance the quality of filming; Kr was added to diminish the discharge threshold. The reactor was filled with the mixture and spark initiation was performed (the discharge energy was 1.5 J). Speed filming of ignition dynamics and FF propagation was carried out from the side of the reactor (Figure S1) with a Casio Exilim F1 Pro color high-speed digital camera (frame frequency of 600 s^{-1}).[15] The video file was stored in a computer memory, and its time-lapse processing was performed.[16] The pressure change in the course of combustion was recorded by a piezoelectric gage synchronized with the discharge. Acoustic oscillations were recorded with a Ritmix sensitive microphone (up to 40 kHz). The audio file was analyzed with the Spectra Plus 5.0 software package. The reagents were of chemically pure grade.

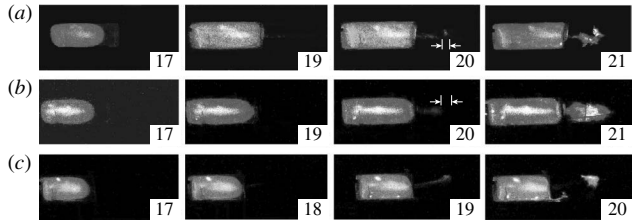

Figure 1 High-speed filming of FF propagation through (*a*) the round opening of 2.5 cm in diameter in a planar obstacle of 14 cm in diameter; (*b*) the round opening of 4 cm in diameter in a planar obstacle of 14 cm in diameter; (*c*) the meshed sphere of 4 cm in diameter (wire diameter of 0.1 mm, cell size of 0.1 mm^2) inserted into a planar obstacle 14 cm in diameter. Initial pressure 170 Torr. The figure on a frame corresponds to frame number after discharge. Arrows specify distances of FF occurrence flame after the obstacle.

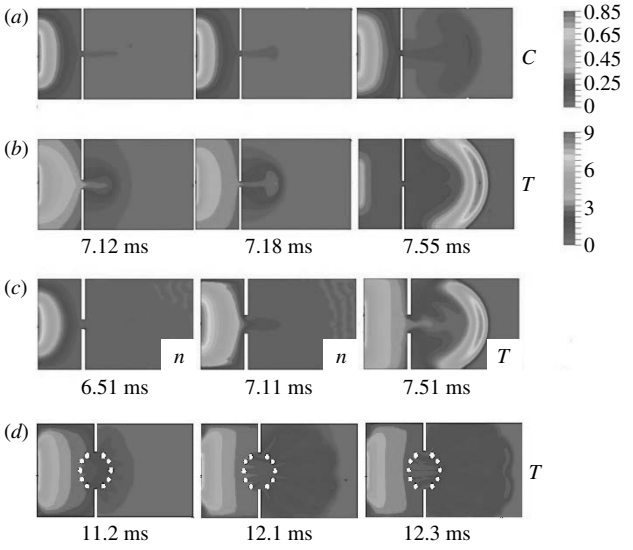

Figure 2 Results of calculation of flame propagation through (*a*)–(*c*) the single opening and (*d*) the meshed sphere. (*a*) Change in the degree of advancement of the reaction and (*b*) the corresponding change in temperature for single Arrhenius reaction; (*c*) change in dimensionless concentration of active intermediate (*n*) and temperature (*T*) for the simple chain mechanism; (*d*) change in temperature for single Arrhenius reaction.

the immediate vicinity of the obstacle, the first spot of ignition is observed considerably far from the obstacle surface. As is seen in Figure 1, the less the diameter of an opening is, the farther FF from an obstacle appears (marked by arrows). A 'flame jump' (by flame jump we mean the distance of flame emergence behind an obstacle) is much longer in the presence of the meshed sphere, as an obstacle [Figure 1(*c*)]. In addition, the flame jump through the meshed sphere can be detected at considerably low initial pressures; besides, under our conditions, the flame in diluted mixture 'jumps' markedly farther than at 1 atm.[9] The establishment of the dependencies of the length of flame jump on the geometry of a complex obstacle needs further investigation. Note that the accumulation of free radicals behind the obstacle was observed experimentally.[9] The mixing of these radicals with the unburned gas leads to a highly explosive mixture.

As a starting point we took a qualitative two-dimensional numerical model of FF propagation through an obstacle using reactive Navier–Stokes equations within a low Mach number approximation. A simple elementary single plain obstacle with a central opening and a spherical meshed one were considered. Note that, in our opinion, any comparison of the experimentally recorded movement of FF with the result of numerical modeling is credible only in a qualitative aspect as there are no unicity theorems on reactive Navier–Stokes equations. Therefore, any agreement between calculated and experimental quantities does not argue for consent between calculation and experiment, as there can be other sets of the governing parameters describing the same experimental profiles (until uniqueness is proved). One can reliably analyze only qualitative velocity changes of movement of the boundary of initial and reacting gas, as well as the shape and perturbations of this boundary. Moreover, a consideration of the detailed kinetic mechanism introduces additional uncertainty into modeling. The vast majority of kinetic parameters is not accurate enough to draw adequate conclusions based on modeling. The question of completeness of the kinetic mechanism is always open, *i.e.* whether any important reaction is overlooked.

Compressible dimensionless reactive Navier–Stokes equations in low Mach number approximation,[15] describing flame propagation in a two-dimensional channel,[16–21] showed a qualitative consent with experiments.[15,19]

The problem was solved by finite element analysis by means of the package (FlexPDE 6.08, A Flexible Solution System for Partial Differential equations, 1996–2008 PDE Solutions Inc.[22]). Initiation condition was taken $T = 10$ on the right boundary of the channel; there was a vertically located orifice in the channel. The boundary conditions were $C_x = 0$, $C_y = 0$, $n = 0$, $u = 0$, $v = 0$, $\rho_x = 0$, $\rho_y = 0$ and convective heat exchange $T_t = T - T_0$.

The results of calculations are shown in Figure 2. The analysis of reactive Navier–Stokes equations in low Mach number approximation allows qualitative describing the experimental features of FF penetration through the obstacle (Figure 1), namely, the occurrence of the FF not in the immediate vicinity of an obstacle but in some distance behind it. Thus, it is enough to analyze the simplest model of a single plain obstacle with one opening for the description of this important experimental feature. The chain mechanism of chemical transformations leads to a better description of the process [namely, the FF movement back to the obstacle after 'flame jump', Figure 2(*c*), frame *T*], as compared with modeling based on a single Arrhenius reaction [Figure 2(*a*),(*b*)]. It means that though the occurrence of 'flame jump' is determined for the most part by the gas-dynamic features of combustible gas penetration through an obstacle, the kinetic mechanism of combustion also considerably influences the process.

Figure 3(*a*) shows the selected frames of speed filming of FF propagation in the gas mixture without obstacles and the time dependence of acoustic oscillations amplitude. In Figure 3(*b*), selected frames of speed filming flame propagation in the gas mixture in the presence of three nested meshed obstacles ($d = 8$, 10, 13 cm) and the time dependence of acoustic oscillations amplitude are presented. The introduction of nested obstacles leads to noticeable frame suppression, as demonstrated by the level of maximum acoustic signal, which is 20 times less in the presence of obstacles than in an empty reactor. It was of interest to determine the dependencies of the maximum acoustic intensity on the number of obstacles.

Note that the influence of obstacles can be expressed in the double way. On the one hand, the FF interaction with an obstacle can cause the development of flame instability, promoting its acceleration. On the other hand, the contact of FF with obstacle surface can increase the contribution of heterogeneous reactions, in particular, chain termination[14] and increase heat losses. In Figure 3(*c*), the dependence of the maximum acoustic intensity on the number of obstacles is shown. Plain obstacles were placed in the center of the reactor at a distance of 2 mm from each other; the spherical ones were nested (13 and 10 cm, 13, 10 and 8 cm, the single obstacle was 13 cm in diameter).

We observed flame acceleration in the presence of a single obstacle as compared with combustion without any obstacle. In these cases, the safety shutter of the reactor swung outward; *i.e.*, the reactor pressure exceeded 1 atm (1.5 atm in the presence of a single obstacle). It does not matter whether the obstacle is planar

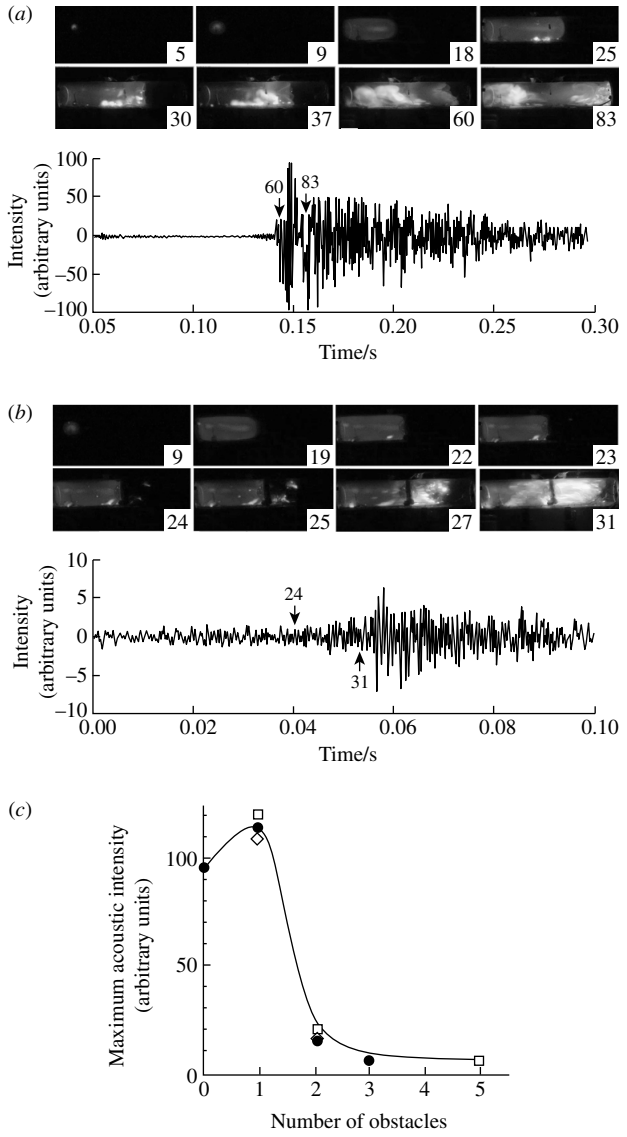

Figure 3 Dependence of effectiveness of flame suppression on the number of obstacles. Initial pressure 170 Torr. The figure on a frame corresponds to frame number after discharge. High-speed filming of FF propagation in the gas mixture in a quartz reactor (*a*) without obstacles and (*b*) in the presence of three meshed obstacles (d = 8, 10, 13 cm) enclosed in each other, spark discharge (1.5 J), speed of filming 600 frames s^{-1}, the first frame corresponds to occurrence of the spark discharge and the time dependence of acoustic oscillations amplitude. (*c*) Dependence of maximum acoustic intensity on the number of obstacles: (●) spherical enclosed obstacles; (□) planar obstacles, d = 14 cm (wire, d = 0.5 mm, cell size of 0.1 mm^2); (◇) planar obstacles, d = 14 cm (wire, d = 0.3 mm, cell size of 0.5 mm^2).

or spherical. However, note that the spherical obstacle consists of two hemispheres (single hemispherical meshed obstacles).

Figure 3(*c*) shows that two or more obstacles strongly suppress flame propagation. In these cases, the safety shutter of the reactor did not swung outward pointing to the fact that the pressure did not exceed 1 atm (<500 Torr according to pressure gage indications). Therefore, Figure 3(*c*) illustrates the occurrence of a boundary (one obstacle) between the flame acceleration and flame suppression modes due to both chain termination and heat losses on the obstacle surface.

The results obtained by the visualization of the development of flame front instabilities are important for the solution of explosion safety problems for volumes with a complex geometry.

Online Supplementary Materials

Supplementary data associated with this article can be found in the online version at doi:10.1016/j.mencom.2015.07.026.

References

1 S. Chakraborty, A. Mukhopadhyay and S. Sen, *Int. J. Thermal Sci.*, 2008, **47**, 84.
2 G. K. Hargrave, S. J. Jarvis and T. C. Williams, *Meas. Sci. Technol.*, 2002, **13**, 1036.
3 I. O. Moen, M. Donato, R. Knystautas and J. H. Lee, *Combust. Flame*, 1980, **39**, 21.
4 S. S. Ibrahim and A. R. Masri, *J. Loss Prev. Proc. Ind.*, 2001, **14**, 213.
5 G. D. Salamandra, T. V. Bazhenova and I. M. Naboko, *Zh. Tekh. Fiz.*, 1959, **29**, 1354 (in Russian).
6 C. Clanet and G. Searby, *Combust. Flame*, 1996, **105**, 225.
7 N. Ardey and F. Mayinger, *Procedings of the 1st Trabson International Energy and Environment Symposium*, Trabson, Turkey, 1996, p. 679.
8 B. Durst, N. Ardey and F. Mayinger, *OECD/NEA/CSNI Workshop on the Implementation of Hydrogen Mitigation Techniques*, Winnipeg, Manitoba, 1996, AECL-11762, p. 433.
9 M. Jourdan, N. Ardey, F. Mayinger and M. Carcassi, *Heat Transfer, Proceedings of 11th IHTC*, Kuongju, Korea, 1998, vol. 7, p. 295.
10 L. A. Gussak, *Turkish M.C. LAG Stratiff. Charge Engines, First Mech. Conference Publication*, London, 1976, p. 137.
11 R. Ch. Abdullin, V. S. Babkin and P. K. Senachin, *Fiz. Goreniya Vzryva*, 1988, **2**, 3 (in Russian).
12 Sh. Yamaguchi, N. Ohiwa and T. Hasegawa, *Combust. Flame*, 1985, **59**, 177.
13 I. M. Naboko, N. M. Rubtsov, B. S. Seplyarskii, V. I. Chernysh and G. I. Tsvetkov, *Fiziko-khimicheskaya Kinetika v Gazovoi Dinamike*, 2012, **13**, URL: http://www.chemphys.edu.ru/pdf/2012-05-30-001.pdf (in Russian).
14 N. M. Rubtsov, B. S. Seplyarskii, I. M. Naboko, V. I. Chernysh and G. I. Tsvetkov, *J. Aeronaut. Aerospace Eng.*, 2013, **2** (5), 1000127 (http://dx.doi.org/10.4172/2168-9792.1000127).
15 I. M. Naboko, N. M. Rubtsov, B. S. Seplyarskii, K. Ya. Troshin, G. I. Tsvetkov and V. I. Chernysh, *Mendeleev Commun.*, 2013, **23**, 358.
16 I. M. Naboko, N. M. Rubtsov, B. S. Seplyarskii, V. I. Chernysh and G. I. Tsvetkov, *Mendeleev Commun.*, 2013, **23**, 163.
17 V. Akkerman, V. Bychkov, A. Petchenko and L.-E. Eriksson, *Combust. Flame*, 2006, **145**, 675.
18 N. M. Rubtsov, B. S. Seplyarskii, I. M. Naboko, V. I. Chernysh, G. I. Tsvetkov and K. Ya. Troshin, *Mendeleev Commun.*, 2014, **24**, 308.
19 C. Clanet, G. Searby and P. Clavin, *J. Fluid Mech.*, 1999, **385**, 157.
20 A. Majda, *Equations for Low Mach Number Combustion*, Center of Pure and Applied Mathematics, University of California, Berkeley, 1982, PAM-112.
21 F. Nicoud, *J. Comput. Phys.*, 2000, **158**, 71.
22 G. Backstrom, *Simple Fields of Physics by Finite Element Analysis*, GB Publishing, 2005.

Received: 27th October 2014; Com. 14/4493